Synthesis, Structure, and Electronic Structure of the Ternary Sulfide $La_7Sb_9S_{24}$

Abdeljalil Assoud, Katja M. Kleinke, and Holger Kleinke*

Department of Chemistry, University of Waterloo, Waterloo, Ontario, Canada N2L 3G1

Received October 11, 2005. Revised Manuscript Received December 12, 2005

A ternary sulfide exists on the quasi-binary section $La_2S_3-Sb_2S_3$, $La_{7+\delta}Sb_{9-\delta}S_{24}$. This material exhibits a small but significant phase range with at least $-0.296(4) \le \delta \le 0.134(6)$. $La_{7+\delta}Sb_{9-\delta}S_{24}$ forms a new structure type, space group $P2_1/c$, with $a = 8.7115(9)$ Å, $b = 14.3450(15)$ Å, $c = 15.2657(16)$ Å, $\beta = 90.105(2)°$ ($Z = 2$) for $\delta = 0.13$. This structure contains chains of severely distorted SbS_5 square antiprisms, interconnected by eight- and nine-coordination La atoms. One position is mixed-occupied by La and Sb, with the La content ranging at least from 57% to 35%. $La_7Sb_9S_{24}$ is a blackish material with a computed gap >1.5 eV.

Introduction

Both binary lanthanum and antimony chalcogenides are under investigation for their potential use as thermoelectric materials.[1,2] This includes not only the telluride Sb_2Te_3,[3,4] which is also a part of the record-breaking Bi_2Te_3/Sb_2Te_3 thin film device,[5] but also the sulfide Sb_2S_3.[6] The same is true for the lanthanum sulfides,[7−10] selenides,[11] and tellurides.[12−14] La_2S_3 in the cubic γ modification (defect $La_{3-\delta}S_4$, $\delta = 0.33$, Th_3P_4 type) was reported to reach a ZT value of 0.5 at 1000 K.[7] Very little comprehensive information about the Ln_2Q_3/Sb_2Q_3 system (Ln = lanthanoid, Q = S, Se, Te) could be found in the literature; aside from vague reports on $La_6Sb_8S_{21}$ and $La_3Sb_3S_{10}$,[15] and the isostructural Ce compounds,[16] the structures of $Eu_3Sb_4S_9$[17] and $Pr_8Sb_2S_{15}$[18] were solved. The lattice parameters of the latter indicate that the so-called "Nd_3SbS_6"[16] might be isostructural. Of these compounds, $La_3Sb_3S_{10}$, most likely a poly-chalcogenide, and $Eu_3Sb_4S_9$ with divalent Eu^{II} are not situated on the quasi-binary section Ln_2Q_3/Sb_2Q_3. On the other hand, a study of the La_2S_3/Bi_2S_3 system revealed the existence of $La_4Bi_2S_9$ and $LaBiS_3$.[19] Moreover, a number of ternary lanthanoid tellurides exist, for example, $LaBiTe_3$, $SmSbTe_3$, and $YSbTe_3$ as revealed via phase diagram studies.[20] We commenced to investigate whether ternary lanthanum antimony chalcogenides may exist with suitable thermoelectric properties. Here, we report on our first finding, a new sulfide situated close to the center of the quasi-binary La_2Q_3/Sb_2Q_3 section, $La_{7+\delta}Sb_{9-\delta}S_{24}$ (with $-0.296(4) \le \delta \le 0.134(6)$).

Experimental Section

Synthesis and Analysis. Our syntheses attempts started from the elements in different ratios, but always with 60 atomic-% sulfur to stay on the quasi-binary La_2S_3/Sb_2S_3 section. The elements were used as acquired and stored in an argon-filled glovebox (La, powder, −40 mesh, 99.9%, Alfa Aesar; Sb, powder, −100 mesh, 99.5%, Aldrich; S, pieces, 99.999%, Alfa Aesar). Initially reactions were carried out aiming at 2:1, 1:1, and 1:2 ratios of La_2S_3:Sb_2S_3. The elements were weighed accordingly and placed into fused silica tubes, which were then sealed under dynamic vacuum. The sealed tubes were heated in a resistance furnace to 800 °C and kept at that temperature for 24 h. After heat-treatment at 700 °C for 7 days, the furnace was switched off to cool to room temperature within a few hours.

Phase identification was performed utilizing the INEL powder diffractometer with position-sensitive detector and Cu Kα radiation. The powder diagram of the ground sample with the 1:1 ratio of La and Sb contains several unidentifiable reflections that also persist, albeit with smaller intensities, in the other two powder diagrams,

* To whom correspondence should be addressed. E-mail: kleinke@uwaterloo.ca.

(1) Tritt, T. M. *Science* **1995**, *272*, 1276−1277.
(2) DiSalvo, F. J. *Science* **1999**, *285*, 703−706.
(3) Dhar, S. N.; Desai, C. F. *Philos. Mag. Lett.* **2002**, *82*, 581−587.
(4) Thonhauser, T.; Scheidemantel, T. J.; Sofo, J. O.; Badding, J. V.; Mahan, G. D. *Phys. Rev. B* **2003**, *68*, 085201/085201−085201/085208.
(5) Venkatasubramanian, R.; Slivola, E.; Colpitts, T.; O'Quinn, B. *Nature* **2001**, *413*, 597−602.
(6) Roy, B.; Chakraborty, B. R.; Bhattacharya, R.; Dutta, A. K. *Solid State Commun.* **1978**, *25*, 937−940.
(7) Wood, C.; Lockwood, A.; Parker, J.; Zoltan, A.; Zoltan, D.; Danielson, L. R.; Raag, V. *J. Appl. Phys.* **1985**, *58*, 1542−1547.
(8) Katsuyama, S.; Tanaka, Y.; Hashimoto, H.; Majima, K.; Nagai, H. *J. Appl. Phys.* **1997**, *82*, 5513−5519.
(9) Hirai, S.; Shimakage, K.; Nishimura, T.; Uemura, Y.; Mitomo, M.; Brewer, L. *Int. Conf. Process. Mater. Prop.* **2000**, *2*, 925−928.
(10) Ohta, M.; Hirai, S.; Kato, H.; Nishimura, T.; Uemura, Y. *Appl. Phys. Lett.* **2005**, *87*, 042106/042101−042106/042103.
(11) Kang, H. R.; Kim, D. C.; Kim, J. S.; McIntosch, G. C.; Park, Y. W.; Nahm, K.; Pelzl, J. *Physica C* **2001**, *364*−*365*, 329−333.
(12) Lockwood, A.; Wood, C.; Vandersande, J.; Zoltan, A.; Parker, J.; Danielson, L.; Alexander, M.; Whittenberger, D. *Mater. Res. Soc. Symp. Proc.* **1987**, *97*, 385−390.
(13) Vining, C.; Wood, C.; Parker, J.; Zoltan, A.; Danielson, L.; Alexander, M. *Proc. Int. Conf. Thermoelectr. Energy Convers.* **1988**, *7*, 9−13.
(14) Danrita, J.; Ramachandran, K. *Ind. J. Pure Appl. Phys.* **1992**, *30*, 747−748.
(15) Gao, J.-z.; Nakai, I.; Nagashima, K. *Bull. Chem. Soc. Jpn.* **1983**, *56*, 2615−2617.
(16) Gao, J.-z.; Nakai, I.; Nagashima, K. *Bull. Chem. Soc. Jpn.* **1984**, *57*, 875−876.
(17) Lemoine, P.; Carré, D.; Guittard, M. *Acta Crystallogr., Sect. B* **1981**, *37*, 1281−1284.
(18) Guseinov, G. G.; Mamedov, F. K.; Amiraslanov, I. R.; Mamedov, K. S. *Kristallografiya* **1981**, *26*, 831−833.
(19) Ecrepont, C.; Guittard, M.; Flahaut, J. *Mater. Res. Bull.* **1988**, *23*, 37−42.
(20) Geidarova, E. A.; Melikova, Z. D.; Sadygov, F. M. *Issl. Obl. Neorg. Fiz. Khim.* **1981**, 131−136.

10.1021/cm052254v CCC: $33.50
Published on Web 01/20/2006

plus weak reflections of the binary sulfide LaS_2 as well as traces of elemental antimony. The other two reaction mixtures contained almost exclusively the unknown phase and La_2S_3 and Sb_2S_3, respectively.

A black block-shaped crystal was selected from the 1:1 reaction for single-crystal structure studies, yielding a refined formula of $La_{7.13}Sb_{8.87}S_{24}$ (for details, see Crystal Structure Determinations). A reaction starting from the elements in this ratio yielded a homogeneous product, $La_{7.13}Sb_{8.87}S_{24}$. Four crystals thereof were analyzed by means of standardless energy dispersive spectroscopy (EDS, LEO 1530, with integrated EDAX Pegasus 1200) using an acceleration voltage of 21 kV. No heteroelements, for example, stemming from the reaction container, were found in any case, and the La:Sb:S ratio was averaged to be 16.7:22.9:60.5 (in at-%). This compares well with the numbers taken from the refined formula $La_{7.13}Sb_{8.87}S_{24}$, that is, 17.8:22.2:60.

To investigate the phase width, a number of reactions were done with different La/Sb ratios, from 4:12 to 10:6 in increments of 1, keeping $\{n(La) + n(Sb)\}/n(S) = 16/24 = 2/3$. Good yields (>80%) were obtained for La/Sb = 6/10, 7/9, and 8/8. One can thus assume that the phase range is between $La_6Sb_{10}S_{24}$ and $La_8Sb_8S_{24}$. Because we already analyzed a sample with an La/Sb ratio of 1:1 (resulting in $La_{7.13}Sb_{8.87}S_{24}$), we investigated the sample with the nominal La/Sb ratio of 6:10. In the end, the crystal structure analysis yielded a refined formula of $La_{6.70}Sb_{9.30}S_{24}$.

Crystal Structure Determinations. Data collections were carried out on a Smart Apex CCD (Bruker) at room temperature utilizing Mo Kα radiation. In both cases, the data were collected by scans of 0.3° in ω in two blocks of 606 frames at $\phi = 0°$ and $\phi = 120°$, with exposure times of 60 s per frame. The data were corrected for Lorentz and polarization effects, and absorption corrections were based on fitting a function to the empirical transmission surface as sampled by multiple equivalent measurements,[21] because the crystal faces could not be determined reliably for numerical absorption corrections.

The data collected from the sample with an equal amount of La and Sb were used for the structure solution utilizing the SHELXTL package.[22] Therein, we quickly identified 9 sites for La and Sb, and 12 for S, corresponding to the general formula $La_{2-\delta}Sb_\delta S_3$. As La and Sb have comparable scattering factors, noting their order numbers of 57 and 51, respectively, we assigned the sites on the basis of the distances to S atoms: the shortest Sb−S distances were expected to be just above 2.5 Å, and the La−S bonds certainly above 2.7 Å. Moreover, the $5s^2$ pair of Sb^{III} is often reflected in a rather irregular coordination around Sb, in contrast to La^{III}. For example, a square SbS_5 pyramid is common among Sb sulfides. On the basis of these criteria, we could clearly identify three La sites (called La2, La3, La4) and four Sb sites (Sb2−Sb5). The ninth cationic site (M1) is unusual, as it exhibits three bonds to S atoms of approximately 2.7 Å, and four distances between 2.94 and 3.36 Å. Refining this site as La yielded a final residual value of R1 = 5.11%, while refining it as Sb resulted in R1 = 5.31. Either way, the U_{22}/U_{11} ratio was around 7, and hence suspicious. Therefore, we decided to refine this site as a split La/Sb position, which led to a decrease in R1 to 4.32%, and a regular U_{22}/U_{11} ratio of 1.4. Because the La1−Sb1 distance is only 0.5 Å, M1 is occupied by either Sb1 or La1. This refinement culminated in 57% La on that site, and a final formula of $La_{7.134(6)}Sb_{8.866}S_{24}$. Correspondingly, the refinements of the crystal taken from the initial La/Sb ratio of 6:10 yielded 35% La on that site, and thus a final formula of $La_{6.704(4)}Sb_{9.296}S_{24}$. The overall smaller La content reflects itself in smaller lattice parameters, for example, a unit cell volume decrease from 1907.7(3) to 1900.3(2) Å^3. Crystallographic details of both data collections are listed in Table 1, and atomic coordinates and displacement parameters of $La_{7.134(6)}Sb_{8.866}S_{24}$ are in Table 2.

Table 1. Crystallographic Data of $La_{7.134(6)}Sb_{8.866}S_{24}$ and $La_{6.704(4)}Sb_{9.296}S_{24}$

empirical formula	$La_{7.134(6)}Sb_{8.866}S_{24}$	$La_{6.704(4)}Sb_{9.296}S_{24}$
formula weight	2839.88 g/mol	2832.50 g/mol
temperature	293(2) K	293(2) K
wavelength	0.71073 Å	0.71073 Å
crystal system	monoclinic	monoclinic
space group	$P2_1/c$ (No. 14)	$P2_1/c$ (No. 14)
a	8.7115(9) Å	8.6829(4) Å
b	14.3450(15) Å	14.3334(7) Å
c	15.2657(16) Å	15.2691(8) Å
β	90.105(2)°	90.078(1)°
volume	1907.7(3) Å^3	1900.3(2)
Z	2	2
density (calculated)	4.94 g/cm^3	4.95 g/cm^3
absorption coefficient	15.27 mm^{-1}	15.16 mm^{-1}
$F(000)$	2486	2480
crystal size [mm]	0.13 × 0.02 × 0.004	0.08 × 0.07 × 0.03
completeness to $\theta = 30°$	99.4%	98.7%
reflections collected	15 686	15 506
independent reflections	5535 [R(int) = 0.0439]	5480 [R(int) = 0.0267]
refinement method	full-matrix least-squares on F^2	full-matrix least-squares on F^2
data/restraints/parameters	5535/0/186	5480/0/186
GOF on F^2	1.051	1.045
R indices ($I > 2\sigma(I)$): R1, wR2	0.0432, 0.0837	0.0286, 0.0631
extinction coefficient	0.00008(2)	0.00056(3)
largest diff. peak and hole	1.87 and −1.79 e/Å^3	2.09 and −2.13 e/Å^3

Table 2. Atomic Coordinates and Equivalent Displacement Parameters[a] of $La_{7.13}Sb_{8.87}S_{24}$

atom	x	y	z	U_{eq}/Å^2
La1[b]	0.1197(2)	0.0900(1)	0.1029(1)	0.0138(2)
La2	0.12863(5)	0.29432(3)	0.32823(3)	0.0132(1)
La3	0.62778(5)	0.28271(3)	0.32866(3)	0.0146(1)
La4	0.63002(5)	0.09757(3)	0.09279(3)	0.0134(1)
Sb1[b]	0.1211(3)	0.0579(2)	0.0937(2)	0.0138(2)
Sb2	0.13232(6)	0.50596(4)	0.17185(3)	0.0135(1)
Sb3	0.36789(7)	0.34858(4)	0.03591(3)	0.0163(1)
Sb4	0.37989(6)	0.03507(4)	0.32423(4)	0.0164(1)
Sb5	0.87837(6)	0.35009(4)	0.05245(3)	0.0140(1)
S1	0.0899(2)	0.5569(1)	0.7434(1)	0.0142(4)
S2	0.1050(2)	0.2905(1)	0.1319(1)	0.0133(4)
S3	0.1258(2)	0.4668(1)	0.4284(1)	0.0143(4)
S4	0.1301(2)	0.6554(1)	0.2515(1)	0.0150(4)
S5	0.1312(2)	0.7942(1)	0.0339(1)	0.0150(4)
S6	0.1689(2)	0.1082(1)	0.4199(1)	0.0130(4)
S7	0.3478(2)	0.4450(1)	0.2610(1)	0.0143(4)
S8	0.3733(2)	0.5325(1)	0.5942(1)	0.0129(4)
S9	0.3841(2)	0.1757(1)	0.2316(1)	0.0150(4)
S10	0.3855(2)	0.3068(1)	0.4729(1)	0.0146(4)
S11	0.5827(2)	0.0988(1)	0.4251(1)	0.0153(4)
S12	0.6498(2)	0.2994(1)	0.1353(1)	0.0140(4)

[a] U_{eq} is defined as one-third of the trace of the orthogonalized U_{ij} tensor. [b] Occupancy f(La1) = 1 − f(Sb1) = 0.567(3) in $La_{7.13}Sb_{8.87}S_{24}$, and 0.352(2) in $La_{6.70}Sb_{9.30}S_{24}$.

Electronic Structure Calculations. Self-consistent tight-binding first principles LMTO calculations (LMTO = linear muffin tin orbitals) using the atomic spheres approximation (ASA)[23,24] were performed. In the LMTO approach, the density functional theory is employed with the local density approximation (LDA) for the exchange correlation energy.[25] The following wave functions were used: for La 6s, 6p (included via the downfolding technique[26]),

(21) *SAINT*, version 4 ed.; Siemens Analytical X-ray Instruments Inc.: Madison, WI, 1995.
(22) Sheldrick, G. M. *SHELXTL*, version 5.12 ed.; Siemens Analytical X-ray Systems: Madison, WI, 1995.
(23) Andersen, O. K. *Phys. Rev. B* **1975**, *12*, 3060−3083.
(24) Skriver, H. L. *The LMTO Method*; Springer: Berlin, Germany, 1984.
(25) Hedin, L.; Lundqvist, B. I. *J. Phys. C* **1971**, *4*, 2064−2083.

5d, and 4f; for Sb 5s, 5p, 5d (downfolded), and 4f (downfolded); and for S 3s, 3p, and 3d (downfolded). The 128 independent *k* points of the first Brillouin zone were chosen via an improved tetrahedron method.[27] Four different models were calculated: for the first two, the $P2_1/c$ symmetry was retained, one with La on M1, thus modeling $La_8Sb_8S_{24}$, the second with Sb on M1, modeling $La_6Sb_{10}S_{24}$. To model $La_7Sb_9S_{28}$, we split the four M1 sites per unit cell into two La and two Sb positions. This can be done in two ways in the monoclinic crystal system, leading to a symmetry reduction from $P2_1/c$ either to Pc (model 3) or to $P2_1$ (model 4).

Physical Property Measurements. We used a two-probe conductivity apparatus designed for pressed powderized samples.[28] Therein, two cylindrical steel stems press onto the sample from two opposite sides, and the resistance *R* is measured between the two stems. As long as the sample resistance is much larger than that of the metallic stems, reliable results are achieved. The specific resistance (resistivity) ρ can be obtained by multiplying *R* with the contact area, πr^2 with $r =$ radius of the stems, divided by the sample height *h*: $\rho = R \times \pi r^2/h$.

Results and Discussion

Crystal Structure. After the successful structure determination of $La_{7.134(6)}Sb_{8.866}S_{24}$ and $La_{6.704(4)}Sb_{9.296}S_{24}$, for simplicity called $La_7Sb_9S_{24}$ hereafter, we postulate that this is the same compound described as $La_6Sb_8S_{21}$ by Gao et al.[15] On the basis of X-ray diffraction experiments, Gao et al. assigned the space group *P*222 with $a = 14.317(2)$ Å, $b = 15.239(4)$ Å, $c = 8.685(1)$ Å, $V = 1895$ Å^3, without actually solving the structure, and the formula was determined with the aid of an electron microprobe analyzer. The lattice parameters are very similar to the ones found here, as listed in Table 1. Scaling $La_6Sb_8S_{21}$ to 24 S yields $La_{6.86}Sb_{9.14}S_{24}$, which is within the phase range determined by us. Hence, Gao's microprobe analysis validates our model of a mixed La/Sb position.

$La_7Sb_9S_{24}$ (Figure 1) crystallizes in its own structure type, with chains of (severely distorted) SbS_5 square pyramids, separated by the La^{III} cations. These chains are interconnected via the four-coordinated Sb1 atoms along the *c* axis to puckered layers perpendicular to the *b* axis.

Such chains are common in antimony chalcogenides, for example, in the binary Sb_2S_3[29] and a number of ternaries, including $K_2Pr_{2-x}Sb_{4+x}Se_{12}$,[30] $Sr_6Sb_6S_{17}$,[31] $PbSb_2Se_4$,[32] $Pb_4Sb_6S_{13}$,[33] $Pb_6Sb_6S_{17}$,[34] $Pb_4Sb_4Se_{10}$,[35] and $Pb_4Sb_6Se_{13}$ and $Pb_6Sb_6Se_{17}$.[36] Part of the countercations (La, K, Pr, Pb) are connected to these SbQ_5 chains, forming larger NaCl-related fragments (ribbons). Most of these structures exhibit a short axis of 4.1−4.4 Å, which is the repeat unit of the chain of edge-condensed SbQ_5 pyramids. $Sr_6Sb_6S_{17}$ is an example where this axis is doubled, like in $La_7Sb_9S_{24}$ with $a = 8.7$ Å, which occurs with the Sb atoms forming zigzag chains along this axis, instead of linear ones. As revealed in Figure 2, some S atoms are also shifted from one unit cell half to the other.

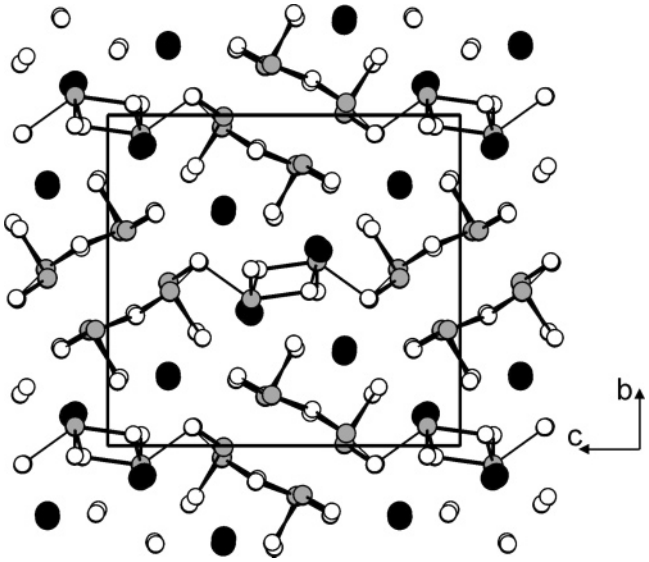

Figure 1. Projection of the structure of $La_{7.13}Sb_{8.87}S_{24}$ along the *a* axis. Large, black circles, La; medium, gray, Sb; small, white, S. La−S bonds are omitted for clarity. Thick contacts, Sb−S bonds < 2.8 Å; thin, <3.0 Å.

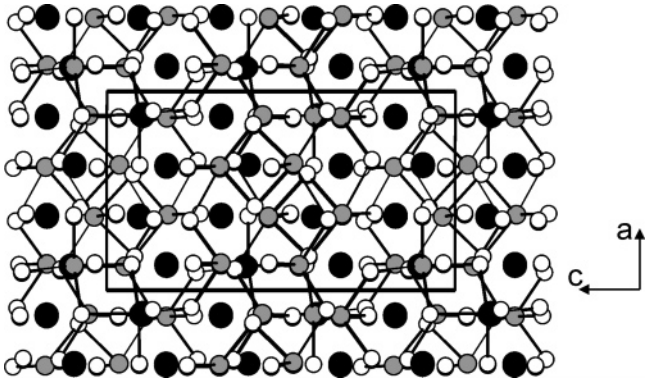

Figure 2. Projection of the structure of $La_{7.13}Sb_{8.87}S_{24}$ along the *b* axis. Large, black circles, La; medium, gray, Sb; small, white, S. La−S bonds are omitted for clarity. Thick contacts, Sb−S bonds < 2.8 Å; thin, <3.0 Å.

Moreover, orthorhombic symmetry is common in these materials, with $Pb_4Sb_6S_{13}$ and $Pb_4Sb_6S_{13}$ (monoclinic space group $I2/m$) being exceptions. As all unit cell angles are close to 90° in the structure of $La_7Sb_9S_{24}$, one might suspect orthorhombic symmetry in this case as well. For example, all heavy atoms lie on $x = 0.13$, 0.38, 0.63, and 0.88 within ±0.01, implying that a mirror plane might exist perpendicular to the *a* axis; however, the positions of the S atoms, for example, S1 and S11, militate against the presence of a mirror plane perpendicular to the *a* axis (Table 2). The same argument holds against the presence of a 2_1 screw axis. We also applied the routine ADDSYM in the PLATON package,[37,38] which showed that no symmetry elements were missing, that is, confirmed the monoclinic space group $P2_1/c$.

(26) Lambrecht, W. R. L.; Andersen, O. K. *Phys. Rev. B* **1986**, *34*, 2439−2449.
(27) Blöchl, P. E.; Jepsen, O.; Andersen, O. K. *Phys. Rev. B* **1994**, *49*, 16223−16233.
(28) Wudl, F.; Bruce, M. R. *J. Chem. Educ.* **1990**, *67*, 717−718.
(29) Kyono, A.; Kimata, M.; Matsuhisa, M.; Miyashita, Y.; Okamoto, K. *Phys. Chem. Miner.* **2002**, *29*, 254−260.
(30) Chen, J. H.; Dorhout, P. K. *J. Alloys Compd.* **1997**, *249*, 199−205.
(31) Choi, K.-S.; Kanatzidis, M. G. *Inorg. Chem.* **2000**, *39*, 5655−5662.
(32) Skowron, A.; Boswell, F. W.; Corbett, J. M.; Taylor, N. J. *J. Solid State Chem.* **1994**, *112*, 251−254.
(33) Skowron, A.; Brown, I. D. *Acta Crystallogr., Sect. C* **1990**, *46*, 527−531.
(34) Orlandi, P.; Meerschaut, A.; Palvadeau, P.; Merlino, S. *Eur. J. Miner.* **2002**, *14*, 599−606.
(35) Skowron, A.; Brown, I. D. *Acta Crystallogr., Sect. C* **1990**, *46*, 2287−2291.
(36) Derakhshan, S.; Assoud, A.; Taylor, N. J.; Kleinke, H. *Intermetallics* **2006**, *14*, 198−207.

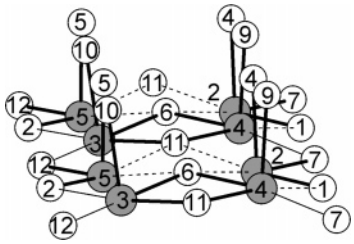

Figure 3. The chain of edge-sharing SbS_5 square pyramids. Thick lines, Sb−S contacts < 2.8 Å; thin, <3.0 Å; dashed, <3.35 Å.

One chain of edge-sharing SbS_5 pyramids of $La_{7.13}Sb_{8.87}S_{24}$ is depicted in Figure 3, formed by the Sb2−Sb5 atoms. The sharing occurs via opposite edges resulting in infinite linear chains along the *a* axis, plus one edge (Sb6 and Sb11) resulting in a double chain of SbS_5 pyramids. Topologically related double chains also occur in, for example, $PbSb_2Se_4$ and $Pb_4Sb_6S_{13}$, in the latter case together with triple chains of SbS_5 pyramids that are the backbone of, for example, $Sr_6Sb_6S_{17}$, $Pb_6Sb_6S_{17}$, and $Pb_6Sb_6Se_{17}$.

Therein, we distinguish between short Sb−S contacts < 2.8 Å, medium (>2.8 Å, <3.0 Å), and long ones (between 3.0 and 3.35 Å). Each of these Sb atoms comprises three short bonds, marked with bold lines in Figure 3, and two longer ones. Hence, one can alternatively view these chains as being composed of trigonal pyramids, as discussed for $Sr_6Sb_6S_{17}$.[31] Such a description clearly shows the need for the presence of two Sb atoms per repeat unit along chain direction, as the short bonds (bold lines) alternate between pointing to the inside and to the outside of the double chain.

Moreover, the Sb−S bonds compare well with the two symmetry-independent Sb sites of Sb_2S_3, where Sb1 forms three bonds to S between 2.52 and 2.54 Å, plus three contacts from 3.11 to 3.17 Å, and Sb2 exhibits three short Sb−S bonds between 2.46 and 2.68 Å, plus two intermediate distances of 2.85 Å, and two long ones of 3.38 Å.[29] In particular, the Sb2, Sb4, and Sb5 atoms of $La_7Sb_9S_{24}$ closely resemble Sb1 of Sb_2S_3, as each of them participates in three short Sb−S bonds between 2.46 and 2.57 Å, with the next shortest contact being larger than 3 Å. The Sb3 atom of $La_7Sb_9S_{24}$ compares well with Sb2 of Sb_2S_3, with three bonds between 2.43 and 2.64 Å, and two longer ones between 2.85 and 2.97 Å (Table 3, values taken from $La_{7.13}Sb_{8.87}S_{24}$).

On the other hand, the Sb1 atom of $La_7Sb_9S_{24}$, the atom on the split position with La1, stands out, as its coordination sphere cannot be viewed as either trigonal or square pyramid. Instead, it resides on top of a S_4 square, with Sb1−S bonds between 2.54 and 2.83 Å. As compared to La1, the environment of Sb1 is severely distorted, reflected mostly in a shift along the *b* axis (vertical in Figure 4). Generally, this situation is reminiscent of the $K_2Pr_{2-x}Sb_{4+x}Se_{12}$ structure with mixed Pr/Sb occupancy (Pr1 and Sb1).[30]

La1 exhibits nine La1−S bonds between 2.79 and 3.45 Å, best described as a capped square antiprism, a coordination polyhedron often found in La chalcogenides. Similarly, the other three La sites, La2−La4, are also nine-fold coordinated in the approximate form of a square antiprism, with La−S bonds between 2.86 and 3.54 Å. For comparison, the shortest La−S bonds in cubic γ-La_2S_3 are 2.93 Å, where

Table 3. Selected Bond Distances [Å] of $La_{7.13}Sb_{8.87}S_{24}$ (Left) and $La_{6.70}Sb_{9.30}S_{24}$ (Right)

La1−S3	2.787(3)	La1−S3	2.780(2)
La1−S3	2.815(3)	La1−S3	2.816(2)
La1−S8	2.826(3)	La1−S8	2.817(2)
La1−S2	2.914(3)	La1−S2	2.887(2)
La1−S1	3.018(3)	La1−S1	3.024(2)
La1−S4	3.252(2)	La1−S4	3.238(2)
La1−S9	3.264(3)	La1−S9	3.261(2)
La1−S10	3.393(2)	La1−S10	3.406(2)
La1−S5	3.447(2)	La1−S5	3.455(2)
La2−S3	2.908(2)	La2−S3	2.939(1)
La2−S2	3.004(2)	La2−S2	3.000(1)
La2−S6	3.035(2)	La2−S6	3.019(1)
La2−S1	3.060(2)	La2−S1	3.046(1)
La2−S7	3.062(2)	La2−S7	3.064(1)
La2−S5	3.094(2)	La2−S5	3.089(1)
La2−S10	3.146(2)	La2−S10	3.144(1)
La2−S9	3.168(2)	La2−S9	3.145(1)
La2−S4	3.243(2)	La2−S4	3.228(1)
La3−S8	2.900(2)	La3−S8	2.924(1)
La3−S12	2.968(2)	La3−S5	2.958(1)
La3−S5	2.970(2)	La3−S12	2.969(1)
La3−S9	3.008(2)	La3−S9	2.991(1)
La3−S11	3.047(2)	La3−S4	3.030(1)
La3−S4	3.048(2)	La3−S11	3.054(1)
La3−S10	3.072(2)	La3−S10	3.057(1)
La3−S7	3.525(2)	La3−S7	3.506(1)
La3−S1	3.544(2)	La3−S1	3.514(1)
La4−S3	2.855(2)	La4−S3	2.874(1)
La4−S8	2.913(2)	La4−S8	2.933(1)
La4−S12	2.972(2)	La4−S12	2.957(1)
La4−S8	3.004(2)	La4−S8	2.996(1)
La4−S10	3.124(2)	La4−S7	3.129(1)
La4−S7	3.132(2)	La4−S10	3.133(1)
La4−S9	3.217(2)	La4−S9	3.201(1)
La4−S5	3.239(2)	La4−S4	3.233(1)
La4−S4	3.270(2)	La4−S5	3.236(1)
Sb1−S3	2.539(3)	Sb1−S3	2.524(2)
Sb1−S3	2.549(3)	Sb1−S8	2.546(2)
Sb1−S8	2.551(3)	Sb1−S3	2.556(2)
Sb1−S1	2.830(3)	Sb1−S1	2.815(2)
Sb1−S2	3.391(3)	Sb1−S2	3.367(2)
Sb1−S4	3.515(3)	Sb1−S4	3.483(2)
Sb1−S10	3.534(3)	Sb1−S10	3.561(2)
Sb1−S9	3.538(3)	Sb1−S9	3.533(2)
Sb1−S5	3.621(3)	Sb1−S5	3.429(2)
Sb2−S4	2.464(2)	Sb2−S4	2.464(1)
Sb2−S7	2.476(2)	Sb2−S7	2.475(1)
Sb2−S1	2.499(2)	Sb2−S1	2.506(1)
Sb2−S2	3.1587(2)	Sb2−S2	3.157(1)
Sb2−S11	3.1840(2)	Sb2−S11	3.170(1)
Sb2−S6	3.315(2)	Sb2−S6	3.309(1)
Sb3−S10	2.433(2)	Sb3−S10	2.428(1)
Sb3−S6	2.552(2)	Sb3−S6	2.553(1)
Sb3−S11	2.636(2)	Sb3−S11	2.649(1)
Sb3−S2	2.846(2)	Sb3−S2	2.819(1)
Sb3−S12	2.969(2)	Sb3−S12	2.967(1)
Sb4−S9	2.463(2)	Sb4−S9	2.458(1)
Sb4−S11	2.513(2)	Sb4−S11	2.504(1)
Sb4−S6	2.574(2)	Sb4−S6	2.570(1)
Sb4−S7	3.000(2)	Sb4−S7	2.997(1)
Sb4−S1	3.104(2)	Sb4−S1	3.127(1)
Sb4−S12	3.446(2)	Sb4−S12	3.444(1)
Sb5−S5	2.455(2)	Sb5−S5	2.447(1)
Sb5−S2	2.468(2)	Sb5−S2	2.464(1)
Sb5−S12	2.470(2)	Sb5−S12	2.468(1)
Sb5−S6	3.298(2)	Sb5−S6	3.277(1)
Sb5−S11	3.307(2)	Sb5−S11	3.298(1)
Sb5−S1	3.401(2)	Sb5−S1	3.429(1)

(37) Page, Y. L. *J. Appl. Crystallogr.* **1988**, *21*, 983−984.
(38) http://web.mit.edu/platon_v40505/platon/docs/platon/pl000401.html.

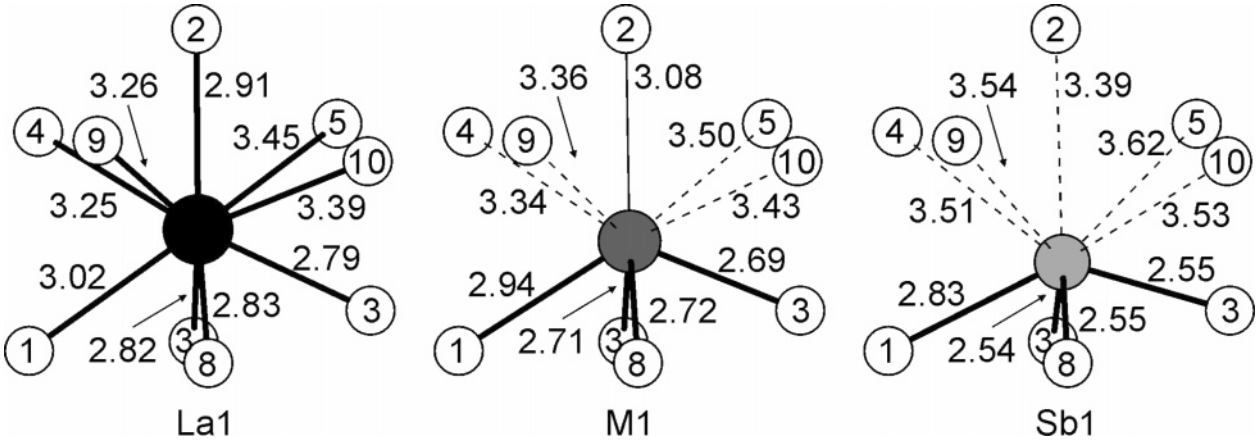

Figure 4. The coordination spheres of La1 (black, left), averaged M1 (dark gray, middle), and Sb1 (grey, right) of $La_{7.13}Sb_{8.87}S_{24}$.

La is eight-fold coordinated by S atoms,[39] and 2.91 Å for both the seven- and the eight-coordinated La atom in orthorhombic α-La_2S_3.[40] The strongly distorted environment of Sb1, combined with the distances to the neighboring S atoms being as short as 2.54 Å, renders the assignment of Sb to that position unambiguous. To further confirm this, we calculated the bond-valences (s) via the Brown−Altermatt approach, where $s = \exp[(r_0 - r)/B]$, with $B = 0.37$ Å, $r_0 = 2.643$ Å for La−S bonds, 2.474 Å for Sb−S bonds, and r being the actual bond distance.[41] Using the Sb radius for Sb1, we calculated a total valence of 3.15, and using the La radius for Sb1 resulted in the unreasonable value of 4.97. Correspondingly, we calculated a valence of 3.38 for the La1 position using the assumed La parameter and an unlikely value of 2.15 using the Sb parameter for La1. Assuming a valence of 3 for these positions, we deduced r_0 to be 2.599 Å for the La1−S bonds, and $r_0 = 2.456$ Å for the Sb1−S bonds. For comparison, the other cationic positions of $La_{7.13}Sb_{8.87}S_{24}$ exhibit calculated valences between 2.84 and 2.97 (La2−La4) and 3.19 and 3.36 (Sb2−Sb5).

Electronic Structure. The computed densities of states for the $La_8Sb_8S_{24}$ and $La_6Sb_{10}S_{24}$ models are shown in Figure 4. The M1 site was assigned to be exclusively La1 in $La_8Sb_8S_{24}$ and Sb1 in $La_6Sb_{10}S_{24}$. Both stoichiometries are just outside of the phase range, and our calculations of the two different $La_7Sb_9S_{24}$ models (in space groups $P2_1$ and Pc, respectively) show intermediate features (see Supporting Information). In either case, the valence band is dominated by the S p block, comprising bonding La−S and Sb−S states, and hence minor contributions of both La and Sb via covalent mixing. The conduction band is composed of the La d and Sb p block.

Like the binary end members La_2S_3 and Sb_2S_3, the ternary $La_7Sb_9S_{24}$ is an electron-precise intrinsic semiconductor. The computed band gap depends slightly on the La/Sb ratio, ranging from 1.70 eV in case of hypothetical $La_8Sb_8S_{24}$ to 1.45 eV in case of hypothetical $La_6Sb_{10}S_{24}$ (Figure 5). The two $La_7Sb_9S_{24}$ models exhibit gaps of 1.55 eV (space group Pc) and 1.50 eV ($P2_1$). Noting that the LMTO calculation utilizing LDA usually underestimates the band gap, and that the material appears to be black, the band gap should be between 1.5 and 1.7 eV.[42] Similar values were determined for Sb_2S_3, with an optical gap between 1.7 and 1.9 eV,[6,43] and the line compound α-La_2S_3 exhibits a slightly larger gap, as it is maroon colored (gap between 1.7 and 2 eV).[44]

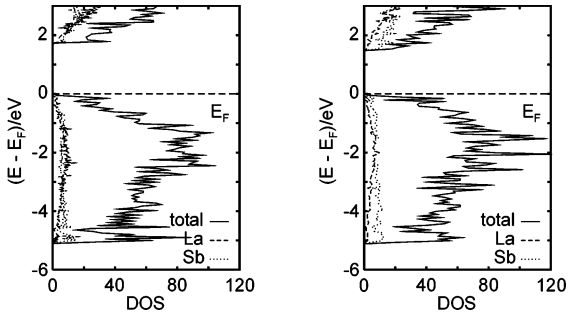

Figure 5. Densities of states of the $La_8Sb_8S_{24}$ (left) and $La_6Sb_{10}S_{24}$ (right) models.

Physical Properties. We were unable to measure the value of the electrical resistance because it was too high to be determined (at room temperature). On the basis of prior measurements, we can deduct the resistivity to be above 1 MΩ cm, not unexpected for an undoped material with a gap >1.5 eV.

Conclusion

A new sulfide, $La_{7+\delta}Sb_{9-\delta}S_{24}$ with $-0.296(4) \leq \delta \leq 0.134(6)$, was synthesized and characterized. Its new structure type comprises chains of SbS_5 square pyramids, interconnected via an additional, four-coordinated Sb atom to puckered layers, separated by the La atoms. The connecting Sb atom shares a split position with La, which can consist of 35−57% La.

The large band gap size impedes the use of this material as a thermoelectric, unless very high temperatures are used. The complexity of the crystal structure, combined with the La1/Sb1 split position, should concur with low thermal

(39) Mauricot, R.; Gressier, P.; Evain, M.; Brec, R. *J. Alloys Compd.* **1995**, *223*, 130−138.
(40) Sleight, A. W.; Prewitt, C. T. *Inorg. Chem.* **1968**, *7*, 2282−2288.
(41) Brown, I. D.; Altermatt, D. *Acta Crystallogr., Sect. B* **1985**, *41*, 244−247.
(42) Nassau, K. *The Physics and Chemistry of Color*, 2nd ed.; John Wiley & Sons: New York City, NY, 2001.
(43) Shutov, S. D.; Sobolev, V. V.; Popov, Y. V.; Shestatskii, S. N. *Phys. Status Solidi* **1969**, *31*, K23−K27.
(44) Gschneidner, K. A., J.; Beaudry, B. J.; Takeshita, T.; Eucker, S. S.; Taher, S. M. A.; Ho, J. C. *Phys. Rev. B* **1981**, *24*, 7187−7193.

conductivity. Thus, investigations of analogous selenides and tellurides, which should exhibit smaller gaps, are in progress. Our preliminary results in the La/Sb/Se and La/Sb/Te systems, however, showed no evidence for the formation of such a material.

Acknowledgment. Financial support from NSERC, CFI, OIT (Ontario Distinguished Researcher Award for H.K.), the Province of Ontario (Premier's Research Excellence Award for H.K.), and the Canada Research Chair program (CRC for H.K.) is appreciated.

Supporting Information Available: Two X-ray crystallographic files (CIF), and one figure depicting the densities of states of $La_7Sb_9S_{24}$ (PDF). This material is available free of charge via the Internet at http://pubs.acs.org.

CM052254V